TOPICAL REVIEW

Motor-commands decoding using peripheral nerve signals: a review

View the article online for updates and enhancements.

Topical Review

Motor-commands decoding using peripheral nerve signals: a review

Keum-Shik Hong[1] , Nida Aziz and Usman Ghafoor

School of Mechanical Engineering, Pusan National University, Busan 46241, Republic of Korea

E-mail: kshong@pusan.ac.kr

Abstract

During the last few decades, substantial scientific and technological efforts have been focused on the development of neuroprostheses. The major emphasis has been on techniques for connecting the human nervous system with a robotic prosthesis via natural-feeling interfaces. The peripheral nerves provide access to highly processed and segregated neural command signals from the brain that can in principle be used to determine user intent and control muscles. If these signals could be used, they might allow near-natural and intuitive control of prosthetic limbs with multiple degrees of freedom. This review summarizes the history of neuroprosthetic interfaces and their ability to record from and stimulate peripheral nerves. We also discuss the types of interfaces available and their applications, the kinds of peripheral nerve signals that are used, and the algorithms used to decode them. Finally, we explore the prospects for future development in this area.

Keywords: neuroprostheses, peripheral nervous system, signal decoding techniques, motor command signals, control

S Supplementary material for this article is available online

(Some figures may appear in colour only in the online journal)

1. Introduction

The mechanical structure of the human hand is very complex, with numerous mechanical effectors, a variety of sensory structures, and a bidirectional interface with the brain. It has 27 degrees of freedom [1] for use in complex grasping tasks, along with a sensory feedback system capable of picking up nociceptive, thermal and tactile information, among other modalities [2]. In the intact human hand, movements are produced by more than 30 muscles positioned within the forearm (extrinsic muscles) or hand (intrinsic muscles). Gripping and gross extension or flexion movements of the whole hand are mediated by extrinsic muscles, mostly innervated by the radial and median nerves. For precise movement and fine movement control of the individual fingers, intrinsic muscles are largely responsible, innervated by terminal branches of the median and ulnar nerves [3].

Loss of an upper extremity can cause devastating impairment for an amputee and can significantly reduce the quality of life. Numerous daily living activities are either no longer possible or require extra time and effort. To tackle this type of severe disability issue, upper limb prosthetic technology has been significantly improved over the last few decades, as a result of technologically improved surgical procedures and scientific advances that have demonstrated the feasibility of neurally controlled prosthetic arms and hands, and interfaces that communicate between a prosthesis and an amputee. Prostheses are becoming ever more sophisticated, with the goals both of improved esthetics (that is, resembling the lost limb as closely as possible) and of feedback and control mechanisms that meet the needs of an amputee.

[1] The author to whom all correspondence should be addressed.

Neural control of a prosthetic arm or hand can in principle be achieved by recording electrical activity from the remaining part of the arm of an amputee. This electrical activity encodes motor command signals that originate in the primary motor cortex (M1) of the brain. These signals are then processed in the spinal cord and travel through the motor nerves to activate specific muscles. In many amputees, even though the muscles are no longer available, the motor signals still exist. Thus, if a missing hand, for example, is replaced by an artificial one, the same motor signals can in principle be decoded to control the prosthesis. It should be possible, therefore, to control a prosthetic arm or hand using a sophisticated brain–machine interface for translation between the amputee's neural command signals and the electric signals that control the prosthesis [4]. These brain signals travel through several modulating and processing units before reaching the target (the residual limb) and can in principle be monitored anywhere along the way. If they are acquired from peripheral nerves of the residual limb, the result is a nerve-signal-controlled interface.

A typical nerve-signal-controlled interface performs three basic processes: recording of physiological signals, decoding of motor signals, and translating peripheral nerve signals into correctly formatted commands to the prosthesis [5, 6]. In the first stage, signals are acquired from the peripheral nerve via a nerve interface [7]. These acquired voltage signals are typically a thousand times smaller than the voltage signals that travel along nerves, and are contaminated with noise generated by muscle contraction, transient effects from the movement of the body, and other sources, and therefore need to be denoised. After denoising, certain features of the signals are extracted to make the resulting data computationally more manageable. These features are then sent to a classifier, decoded into motor signals and used to drive the prosthetic limb. A block diagram illustrating the pathway from nerve interface to prosthesis actuation is shown in figure 1.

It depicts an interface linking activity in the median, ulnar, or radial nerve from the residual limb of a patient to movement of a prosthetic device.

Over the last two decades, research has been carried out on a variety of interfaces [8], translation algorithms [9, 10], and prosthetic limbs with near-to-natural operation and aesthetics. Motor signals from peripheral nerves can be acquired using various types of interfaces that are either placed inside the nerve fascicles (intra-neurally) or around the periphery of a nerve (extra-neurally). Intra-neural interfaces are usually used to record action potentials (spikes), while extra-neural interfaces are used to record population activity signals. For decoding movement intent, raw motor signals or action potentials directly from the peripheral nervous system (PNS) are rarely used. Several signal conditioning steps are usually required to formulate appropriate commands. First, the motor signals are filtered to remove noise, and their complexity is reduced using dimensionality-reduction algorithms. The next step in a typical intra-neural interface is to extract and sort different types of spikes according to their shapes, amplitudes, and firing rates. The extracted signals are then classified using classification algorithms. A similar procedure is used for extra-neural interfaces, except that the features are extracted from population activity signals rather than individual action potentials. The decoded output signals from these interfaces are then forwarded to drive the prosthesis.

The purpose of this paper is to review state-of-the-art techniques for acquiring motor signals from peripheral nerves, and the algorithms that are used to decode this high volume, non-linear data for formulation of commands that can be used to drive a prosthetic limb. Figure 2 presents the methods discussed in this paper. Recording interfaces for cortex, muscle and nerve are discussed in section 4, with the focus on peripheral nerve interfaces. Studies of state-of-the-art peripheral nerve interfaces usable in humans are discussed in section 5, along with their limitations. Peripheral nerve signal decoding algorithms and performance evaluation methods are discussed in sections 6 and 7, respectively. Section 9 explores possible and desirable future developments in the technology of nerve interfaces and decoding schemes.

2. Motor system physiology

The human nervous system consists of the CNS (central nervous system); made up of the brain and the spinal cord, and the PNS, made up of peripheral nerves and a variety of other components such as the autonomic nervous system. This review is focused mainly on interfaces and decoding schemes related to the peripheral nerves, hence in this section we narrow our scope to the PNS and motor signals only.

Each peripheral nerve contains a group of fascicles—small bundles of nerve fibers. The nerves are organized somatotopically and functionally at the fascicular level [11]. Different fascicles within a nerve eventually branch off to distinct targets. Fascicular groups destined for nearby targets remain clustered within the nerves over long distances, thus facilitating selective interfacing with specific fascicles within a given nerve. For example, the nerves innervating a muscle in the upper arm have their cell bodies in a vertically oriented column inside the spinal cord, and their axons leave the spinal cord through the ventral roots, sometimes from multiple segments. These axon fibers then regroup distally, until all axons innervating a specific muscle are grouped together in one fascicle of the nerve. The fascicles may contain axons arising from motor, sensory and autonomic neurons. Of these, two types of axons are important for controlling prosthetic limbs: efferent (motor) and afferent (sensory) fibers. The motor nerves carry efferent signals from the brain via the spinal cord to the designated muscle to drive movement. In the other direction, the sensory nerves carry afferent signals from the skin back to the brain, via the spinal cord, dorsal root ganglia and brainstem; in this way tactile stimuli picked up by the skin can influence brain activity [12, 13]. Golgi tendon organs and muscle spindles are responsible for sending proprioceptive feedback (joint motion and position). Autonomic nerves control involuntary and semi-voluntary functions such as heart rate, blood pressure, digestion, and sweating.

Voluntary movements are planned and executed by the central nervous system. For determining motor intent, neurons (and their axons) are the main sources of meaningful
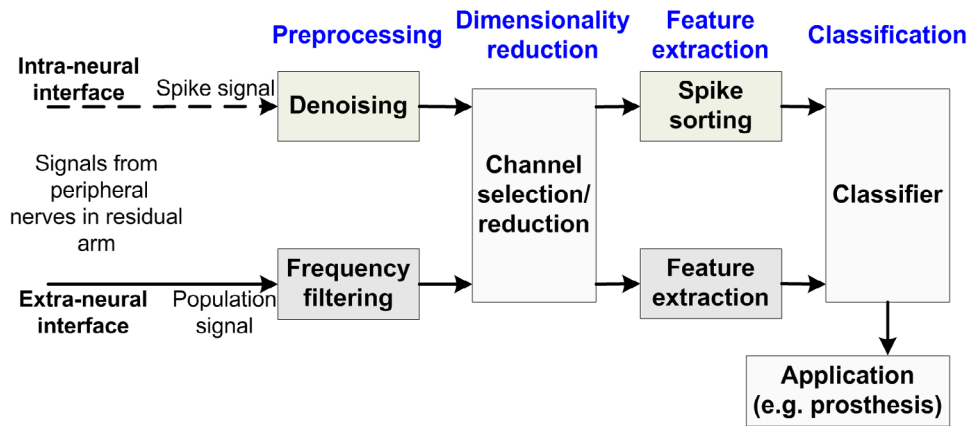
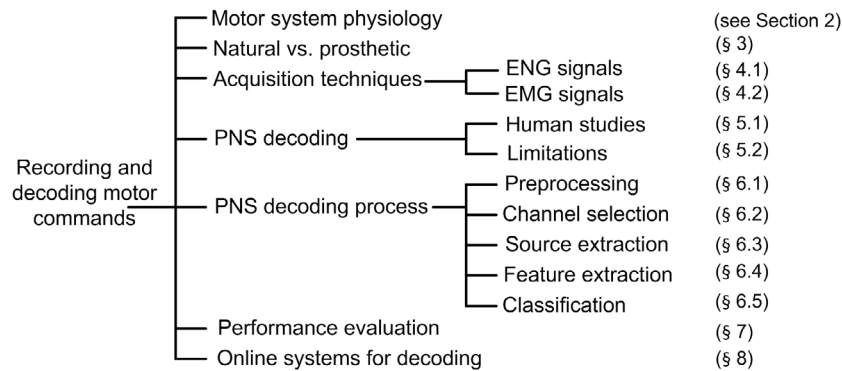**Figure 1.** General framework for a prosthetic interface.

Figure 2. Breakdown of methods for recording and decoding peripheral nerve signals.

signals, with other cells such as glia providing little or no useful information. When a person intends to move a body part, an electrochemical reaction takes place in the motor cortex of the brain. As a result of this reaction, neurons fire action potentials, which are approximately 150 mV changes in the electrical potential within the neural cell relative to the outside, and which last for approximately 1 ms [14]. Each motor neuron has an axon, a thin fiber that projects from the cell body, which can propagate action potentials to other neurons or to distal muscles and organs. Action potentials affect other cells, including muscle cells, via synaptic connections. In this manner, signals (motor commands) travel through the CNS to reach the proximal ends of peripheral nerves that are connected to target muscles. As a result, the muscles execute contractions. Interfaces placed either inside or around the nerves can record voltage signals representing the neuronal activity in the surrounding axons. Thus, nerve signals can be recorded via various types of interfaces and then decoded for determination of a person's intent.

3. Natural versus prosthetic

The human hand is a vital and complex body part, performing a wide range of functions, from opening doors to operating complex machinery. It allows precise control of the grip patterns required for various tasks and the amount of force required to perform them [3]. Losing a hand can have devastating effects on a person's life, in many cases making the amputee dependent on others for even the most basic tasks such as eating. Over the last few decades, a great deal of research has been carried out to create prosthetic hands that look and perform like natural hands. There have been many advances in the mechanical structure, number of degrees of freedom, smoothness, and stability of prostheses such as the BeBionic® and Ottobock®. Even so, a large gap remains between natural and prosthetic hands in terms of control and feedback. Farina and Aszmann [15] noted the following major requirements for better performance: (i) Better peripheral nerve data-recording interfaces and decoding of user intention; (ii) Development of algorithms that do not require the individual to concentrate on trying to move the prosthesis. (An intact person requires no concentration; rather, hand movement is accomplished subconsciously, which frees the brain to take other actions.) (iii) Provision of crucial sensory inputs to the brain. (The natural hand can feel sensations including pressure, temperature, and texture.) (iv) Closing of the loop by providing feedback. (Pressure sensation helps the subject generate the correct amount of force to grasp each specific object.)

The use of signals from peripheral nerves can address some of these needs to a degree, and is thus categorized as an alternative method for signal acquisition, as a substitute for the use of cortical or muscular signals [16]. To be sure, it is impossible to acquire useful PNS signals from tetraplegic patients, who require other types of solutions. However, in cases of trans-humeral or trans-radial amputation, PNS signals can be attained from the residual limb and used to control

prostheses. An additional consideration is that, as alluded to above, amputees may be psychologically disturbed after going through traumatic event: therefore, asking brain surgery for the purpose of recording motor signals to drive prostheses seems inappropriate. In such cases, acquiring signals from the PNS may be a more suitable option, and may also be less painful for the patient. This can be viewed as one of the advantages of PNS signals. The pros and cons of PNS signals with respect to different types of interfaces are discussed further in the next section.

4. Acquisition techniques

Since our focus is on PNS signals, only a brief description of the techniques employed for detecting usable motor commands from the brain is presented. In-depth descriptions are reserved for interfaces and techniques for PNS signal acquisition.

One potential source of information for acquisition of motor signals is the brain itself. The brain is an especially useful source in cases where the patient suffers from high spinal cord paralysis, locked-in syndrome, or severe communication disorders. In these situations, signals from muscles and proximal nerve endings are unavailable because no signals reach these points [17]. Signals originating in the motor cortex of the brain can be acquired either non-invasively or invasively. Several cortical interfaces have been designed and tested for detection of these motor commands. Noninvasive techniques can detect specific signals of brain activity and interpret them to generate control signals. Various modalities can be used for recording, including electric potentials (via electroencephalography) [18–22], neuromagnetic signals (via magnetoencephalography) [23] and concentration changes in oxy- and deoxy-hemoglobin (via functional near-infrared spectroscopy) [24–32]. These signals are preprocessed for removal of physiological noise and passed to pattern-recognition algorithms to decipher the user's intent [33–35]. The existing noninvasive techniques are unidirectional: it is possible to acquire signals from the brain to using them for prosthesis, but it is much more difficult to send usable feedback to the CNS. Cortical signals can also be obtained by invasively placing interfaces directly into the cortex via surgery (see further details in [36]). These interfaces can detect more natural and less noisy signals, either in the form of spikes or of population activity signals. Having higher peak values and a better signal-to-noise ratio (SNR), cortical signals have been successfully used to decode user movement intent; however, many users may be reluctant to adopt this approach due to the requirement of brain surgery.

For this reason, many research groups have begun working on alternative techniques for attaining motor control signals. Peripheral nerve signals are qualitatively very different from cortical signals but are nevertheless useful for decoding user intentions. In the following section, we discuss the state of the art in PNS signal decoding.

4.1. Signal acquisition techniques for peripheral nerves

Myoelectric, body-powered, and hybrid type prostheses are widely used for individuals with upper limb loss [17]. Surface electromyogram (EMG) signals from residual limb muscle sites are used to control motors in myoelectric prostheses. They are usually controlled by recording weak and strong contractions of either one muscle or two independent muscles. In body-powered prostheses, large mechanical structures are involved. To generate the necessary force, amputees can apply their remaining shoulder movements via a harness and cable that is connected to the terminal device, elbow, or wrist. Users of this type of prosthesis can switch functions (locking and unlocking of the joints) by pressing a toggle switch or by pulling a locking cable. Because these types of prostheses do not require surgery, they are acceptable to most users even though the control is not very intuitive [37]. In general, reduced prosthesis weight is the highest priority design concern of users, with sensory feedback and better dexterity following in importance.

Another emerging type of prosthesis, making use of peripheral nerve interfaces, has gained increasing attention over the last 20 years. The basic principle lies in recording motor signals from peripheral nerves and sending back sensory information through electrical stimulation. When cortical signals reach the proximal end of the nerve (after processing at several way-stations, notably the spinal cord) and are recorded, they are called electroneurographic signals (ENG). These signals can be intercepted by placing interfaces either on the nerve (extra-neurally) or within the nerve (intra-neurally).

4.1.1. Extra-neural interfaces. The range of peripheral nerve interfaces can be split into two broad categories, extra-neural and intra-neural. An extra-neural interface surrounds a peripheral nerve. These interfaces do not breach the protective sheath of the nerve, thus are less invasive than intra-neural interfaces. The initial designs of this type were helical and spiral [38, 39]. A simpler form is a cuff-type interface that contains multiple distinct electrodes for recording of population activity around the periphery of the nerve. However, the circular shape has the shortcoming of minimal interaction with specific neurons or axons, hence low selectivity. Since the interface and nerve are separated by a protective sheath, recording of individual nerve fibers is not possible [8]. Multiple cuff interfaces can be placed on different nerve branches close to the end organ to achieve better selectivity, but at the cost of increased implantation risks.

Recording neural activity with nerve cuff electrodes provides several advantages in terms of safety, non-invasiveness, and selectivity, as compared with intra-neural interfaces. An upgraded version of this type of interface was introduced in 2002 by Tyler and Durand [40], named the flat interface nerve electrode (FINE). This was developed to increase the contact area of the interface with the nerve without penetrating it. The FINE gently flattens the nerve to make the inner fascicles more accessible. However, the individual efferent and

afferent fibers remain inaccessible [17]. The amplitude of the action potentials detected by extra-neural interfaces is much lower than in the case of intra-neural interfaces and depends on the distance of the electrodes from the active axons [12]. Extra-neural interfaces have been widely applied in acute studies of motor behavior, for recording and stimulation of peripheral nerves of cats [38, 39, 41, 42], rabbits [9, 43, 44], dogs [45, 46], rodents [47], human models [48], and human subjects [49–54]. Previous work [55] on the development and implementation of FINE has achieved many breakthroughs, including (i) a high degree of selectivity, as estimated by individual fascicle recording; (ii) use of blind source algorithms to decode motor commands; and (iii) (by employing arrays of interfaces along the peripheral nerve) excitation of fibers having small diameters before large fibers, thereby reversing the usual recruitment order. FINE and spiral cuff interfaces have been implanted in humans with limb loss for periods as long as 4 years, maintaining stability and selectivity [51, 52].

4.1.2. Intra-neural interfaces. Intra-neural or intra-fascicular interfaces are physically inert electrical contacts placed inside nerve fascicles, so that they come into direct contact with axons. Both efferent and afferent axons can be reached, so recording of motor commands is not difficult. Higher recording selectivity and better SNR can be achieved than with cuff electrodes [8, 47, 56]. The first intra-neural interface, developed in 1989, was a single-channel Pt-Ir wire designed for small nerve fascicles [57]. It was inserted into a fascicle to obtain a neural signal with high SNR and greater selectivity. With technological advances, micro-machined interfaces are now available with more channels and contacts. Among the available intra-neural interfaces, the longitudinal intra-fascicular electrode (LIFE) [58], a conducting wire implanted longitudinally parallel to a nerve fascicle, is potentially very interesting due to its selectivity and relatively low level of tissue damage. After testing of biocompatibility and efficacy in experimental models, the LIFE has been implanted in humans for decoding and stimulation [59–61]. Successful recordings of voluntary motor commands were achieved, along with evoked sensations of touch, joint movement, and position. The human subjects were able to control a prosthetic arm, and to improve their performance with experience and training.

A variant of the LIFE is the thin-film longitudinal intra-fascicular electrode (tfLIFE), a micro-machined bio-compatible electrode designed to be more flexible and to allow use of more active electrode channels and sites than the original LIFE. The tfLIFE has been tested in the sciatic nerve of rats for periods of up to 3 months [62]. The possibility of decoding motor commands suitable for dexterous control of a hand prosthesis was investigated using the tfLIFE, showing that motor information, grip types, and single finger movements could be extracted with a classification accuracy above 80% [63, 64]. Moreover, a bidirectionally controllable prosthesis was successfully achieved [65] in a person with an amputation.

Another type of penetrating interface is the transverse intra-fascicular multi-channel electrode (TIME) [66], which has aligned contacts inserted perpendicularly to the nerve. These interfaces have a larger number of channels (up to 16), higher selectivity [67], and better biocompatibility [68, 69]. An acute stimulation and recording study in pigs using both TIME and tfLIFE found that TIME interfaces were able to recruit more muscles with higher selectivity than tfLIFE interfaces [70]. In that study, sequences of electric stimuli were applied to individual contacts. Several pioneering studies using LIFE interfaces have demonstrated the possibility of recording and stimulation of peripheral nerves in various animals and models [71–78]. A real-time bidirectional hand prosthesis control using TIME has also recently been demonstrated [79].

Another family of penetrating intra-fascicular interfaces are known as microelectrode arrays (MEA) [80–82] or multiunit arrays (MUA) [83, 84]. Among these devices, the most popular is the Utah slanted electrode array (USEA) [85–88], which consists of 100 needle-shaped electrodes arranged in a 10×10 matrix. This type has varying electrode densities, matching several designs proposed in the literature, with multiple penetration depths. Each needle is less than 80 μm in diameter, and the needles vary in length from 0.5 mm to 1.5 mm [89]. Flexible penetrating microelectrode array interfaces [90] have also been developed recently, to demonstrate their viability for extracting sensorimotor information from the peripheral nerves. These interfaces have great benefits for individuals who have suffered a limb loss, but an increased risk of nerve damage because they are inserted perpendicularly to the nerve. Thus, the USEA offers higher selectivity than LIFE, tfLIFE or TIME but is more invasive. Due to their proximity to the axons, MEAs are capable of isolating individual action potentials; therefore, a small group of axons can be selectively recorded. One of their disadvantages, however, is a tendency to damage the nerve, which reduces long-term stability.

4.1.3. Regenerative interfaces. Regenerative interfaces generally comprise a sieve or array of micro-channels [91]. After the device is inserted into a transected nerve, axons can grow through the holes and make functional connections with electrical contact sites. Differences in the growth rates of axons through the holes can permit selective stimulation and make it possible to record action potentials from individual axons or a small group of axons. Ideally, each axon should pass through a hole individually, resulting in very high selectivity for recording or stimulation. By reducing the size of the sieve, with a corresponding increase in the number of fine holes [92], a greater number of selective recording sites can be obtained. This is the most invasive of all the interfaces that have been discussed but has the highest selectivity. The most exciting application of these interfaces will be implantation in the severed nerves of an amputated limb for bidirectional control of a prosthesis [6]. These interfaces can only be applied to transected peripheral nerves and require time for regenerating axons to grow through the holes, and thus do not allow acute experiments [93]. This can be considered a drawback, in that useful motor control can only be achieved after several months. Although promising results on the use of regenerative interfaces have been achieved in experimental models [94, 95], challenges remain that currently limit their clinical usability.

4.2. Signal acquisition from muscles

The peripheral nerves culminate in the muscles, where the neural signal is, in a sense, transformed and amplified to create the EMG signal. This signal can be detected by placing a type of interface known as an implantable myoelectric sensor (IMES) [96], either invasively into the muscle or non-invasively on the skin surface. The prescribed method of acquisition and decoding of the EMG signals to control a prosthesis includes the following steps: (i) signal conditioning; (ii) pre-processing; (iii) extraction of features; (iv) dimensionality reduction; (v) pattern recognition; (vi) learning (offline and online) [97]. Surface and intramuscular EMG electrodes are discussed further in the following section.

4.2.1. Surface EMG electrodes.
The focus of this review is on peripheral nerve interfaces, but a brief account of EMG-based decoding and interfaces is useful for comparative purposes. The EMG is a significant source of information, potentially allowing an amputee to control a prosthesis without requiring implantation of an interface within a nerve or muscle. The signals can be acquired using non-invasive surface electrodes positioned over the muscles. The most primitive example of such an interface is an on-off control: when a certain EMG signal exceeds a specified threshold, a specific prosthesis function is activated [98]. It is easier to acquire signals in this way than by using peripheral nerve interfaces. In the past, several designs have been proposed, including high-density surface EMG [99] and multi-channel surface EMG [100]. Several experiments have been conducted to validate these approaches to prosthesis control, both in virtual and real environments [101]. However, EMG signals can be recorded only if a substantial volume of muscle is available at the amputation site. Even then, it is generally not possible to use homologous muscles to control the prosthetic device; this limitation makes the interface feel unnatural. This in turn requires a great amount of mental effort and concentration from the user to control the prosthesis. Moreover, the recorded signals do not reflect the contributions of deeper muscles, are affected by displacement of the muscles during contraction, and suffer from cross-talk between muscles. For these reasons, several researchers have begun working on invasive EMG and peripheral nerve interfaces.

4.2.2. Invasive EMG.
Research on invasive EMG interfaces is motivated by the varying and inconsistent motor signals from surface EMG electrodes, which lead to high rates of prosthesis rejection by users. Surface electrodes are impacted by phantom limb sweating, meager contact with the skin, and their ability to record signals only from superficial muscles, whose function often does not relate to the intended prosthetic application [102]. To overcome these issues, along with the problems of muscular crosstalk and displacement, intramuscular EMG recording has been proposed as an alternative to surface EMG. Implantable myoelectric sensors (IMES) are small electrodes designed to sense and transmit EMG signals wirelessly to a prosthesis. They were designed for simultaneous recording of signals from multiple amputated limb muscles, with the goal of allowing natural-feeling control with several degrees of freedom. Recently, IMES electrodes have been successfully implanted in an amputee to control a prosthetic hand in a stable and intuitive way. Furthermore, single channel [103] and multi-channel intramuscular [75] thin-film electrodes have been designed and tested *in vivo* in humans for detection of muscle signals [104]. These electrodes have been extensively tested in deep and superficial muscles. The accuracy of control of a prosthesis was significantly improved using IMES. The results of earlier studies showed that recording of the voluntary activity of individual muscles and transmission of this information wirelessly can be used to control a prosthetic device with three degrees of freedom, namely, wrist supination/pronation, finger extension/flexion, and thumb abduction/adduction. However, if the target muscle sites are located very close together or are very small, then IMES are not useful for detection and decoding of control commands.

5. State of the art in PNS decoding

Peripheral nerve interfaces are critical components required for bidirectional control of a prosthesis from the residual arm of an amputee. Their effective development requires careful consideration of neural anatomy, molecular biology, and physiology. Successful development and clinical utilization of extra- and intra-neural interfaces has significant benefits on those who have lost limbs. As the technology improves and understanding of the relevant physiology increases, selective interfacing at the neuronal level has drawn increasing attention as a means of allowing an amputee to dexterously control multiple degrees of freedom. However, additional studies are still needed of the long-term use of peripheral nerve interfaces. For complete success, the biocompatibility of interfaces must be upgraded to the level needed for long lasting and stable communication.

As alluded to above, if volitional motor commands to the hand can be detected, they can be used to control a prosthesis [105]. The control of an electroneurographic (ENG)-based prosthesis is based on a fundamental principle: movement related activity may remain present in the motor cortex of the brain [106] and the peripheral nerves of an amputee.

5.1. Human PNS decoding

Several recent experimental studies have demonstrated the viability of restoring sensory feedback and intuitive control of multiple degrees of freedom in upper limb amputees using prosthetic devices driven by PNS signals.

In the first human study, eight amputees were enrolled for implantation of intra-neural interfaces (LIFE) percutaneously in severed peripheral nerves for two days, to record volitional motor commands and to provide sensory information (touch and proprioception) by electrical stimulation with varying current intensity [59]. In follow-up work, the same researchers demonstrated for the first time the bidirectional control of a prosthesis in the absence of visual feedback [60]. The amputees could set a gripping force, and joint position feedback

was given to them using electrical stimulation. The amputees performed well due to continuous short-term training after the implant surgery, resulting in improved volitional control of prosthesis activity. The sensory stimulation parameters remained stable over time and provided discrete or graded sensations of touch or pressure encoding joint-position information [107].

Another important study, showing the possibility of obtaining motor signals from the median nerve of the left arm (though not in an amputee), was published in 2005 [108]. MEAs were implanted in a healthy volunteer for the period of approximately three months. This pilot study demonstrated the compatibility, efficiency and long-term operability of the implanted interface, with simultaneous real-time control of a hand prosthesis and electrical stimulation of the peripheral nerve as feedback. No discernable loss of motion control or hand sensation was experienced by the subject, and no signs of infection were found when the implant was removed.

In 2007, a study of the feasibility of detecting motor control signals from long-term amputees was conducted using three intra-neural interfaces, implanted in the median, ulnar and radial nerves [109]. The amputees were able to generate volitional motor nerve potentials that related to the movement of the residual limb. Finger extension/flexion, wrist extension/flexion, and forearm supination/pronation signals were successfully decoded and used to drive the prosthesis.

In 2011, intra-neural interfaces (tfLIFEs) were implanted in the median and ulnar nerves of an amputee to record motor commands that were usable for controlling a prosthesis [64]. Several algorithms were used to decode the commands (single finger movement and grip types) for dexterous control of the prosthesis with 85% accuracy. Extending this work in another study, the same researchers were able, by implanting flexible intra-neural interfaces (tfLIFE4) in a peripheral nerve, to achieve real-time control of three hand movements using distinct motor commands [65]. Although the stimulation thresholds for sensory feedback were not stable 10 d after surgery, control of multiple movements of the prosthesis was successfully achieved.

In 2014, a newly designed intra-neural interface (TIME) was implanted in a peripheral nerve of an individual having an upper extremity amputation [79]. This interface was able to provide stable, bidirectional, and nearly natural control of a prosthetic device together with tactile feedback over the study period of one month. Sensory information from the sensor-equipped hand was transferred to the individual using electrical stimulation. This real-time interface was able to control various grasping movements without requiring audio or visual feedback. Furthermore, three different levels of the force were distinguished using a surface EMG interface, and consistently used by the subject.

In a parallel study in 2014, a new mechanism of communicating with prosthetic devices was proposed by a research group. They provided a long-lasting, stable, reliable, and bidirectional interface between a prosthesis and an individual with a trans-humeral amputation [54]. Several epimysial EMG electrodes were implanted in subjects to record motor commands, and cuff-type interfaces surrounded a peripheral nerve

for sensory stimulation. Repeated sensory perceptions similar in quality, magnitude, and localization were produced, along with precise and intuitive control of the osseointegrated prosthetic device, for more than one year. A total of eight different movements of the hand were controlled with an accuracy of more than 90%. All the tests were carried out with amputees while they were performing daily activity tasks.

More recently, a highly penetrating USEA interface was implanted for a month in two subjects having upper limb extremity amputations [89]. The subjects were able to control individual fingers of a virtual prosthetic hand. Two movement commands were decoded successfully online and 13 were decoded offline. This interface has the potential to access many neurons, and therefore in principle can selectively evoke more than eight sensory percepts of different hand locations and can control high degree-of-freedom prosthetic limbs.

Besides the above-mentioned studies, several notable experiments have been performed on methods of achieving sensory feedback. Stable and selective sensory perceptions without tingling or paresthesia were achieved for more than 3 years in a chronic human experiment using an implanted extra-neural (FINE and cuff) interface [52, 53]. Consistent thresholds and impedances were recorded during the study period, which made use of distinct perceptual areas on the residual limb of an amputee. However, aspects related to prosthesis control were not evaluated in these long-term implant studies. This review has made attempts to circumvent information related to sensory stimulation and its characteristics using peripheral nerve interface.

5.2. Limitations in long-term use of state-of-the-art PNS acquisition techniques

Longevity, biocompatibility (tissue response), mechanical durability, and functional stability are essential aspects of neural interfaces [14, 105]. In an ideal case, useful recordings would be maintainable for many years from the peripheral nerve interfaces, and the measured activity from the nerve would provide stable signals over the life of the interface. A good interface should have the following features: (i) selective recording of the target neurons, (ii) specifically designed and fabricated for peripheral nerve; (iii) mechanically durable; (iv) able to communicate bidirectionally; (v) functionally stable in electrical terms; (vi) able to resist damage by foreign body reactions; and (vii) (the most important factor) capable of biointegration, i.e. biocompatible. Two types of biocompatibility come into play for implantable interfaces: passive and active [56]. Passive biocompatibility is related to the reaction of tissues to the shape, composition, and mechanical properties of the interface materials, while active biocompatibility is related to the operating performance of the interface. Inflammation and tissue response (fibrosis) play a critical role in reducing the performance of the interface. The control of implantation site responses (inflammation) is crucial for long-term stability of an implant [110]. This can help in maintaining neurons near the implanted interface. Inside the nerve, the more biocompatible the interface, the more the space between recording interface and the neurons can be reduced, with neuronal

growth towards the interface. Management of inflammation can improve long-term stability, both from the device standpoint and the neural-network standpoint. Several techniques to minimize interface-associated inflammation are described in the literature, including coating the interface with an adhesive or conducting polymer, reducing stiffness, and the use of anti-inflammatory surfaces.

Various interfaces have been implanted in animals to check their biocompatibility and recording/stimulating capabilities [62, 68]. In a chronic study of cats, intra-neural interfaces (USEAs) were implanted for the period of 12 months [88]. The researchers examined the foreign body response to the implanted interface and its surrounding cuff. Increased numbers of activated microphages were observed at the implantation site and distal to the implant. The results provided evidence of axons around the interface, and a compensatory regenerative response after the initial injury of the nerve was also observed.

More recently, the long-term viability of an implanted intra-neural interface (TIME) was demonstrated in rats [111]. The results showed that the stimulation thresholds and impedance of the interface were increased moderately during the first month but remained stable for the rest of the study period (5 months), despite the presence of a foreign body reaction. Over time, fibrous tissues developed and surrounded the neural implant, resulting in an increase in the diameter of the nerve. In addition, it was found that the density of neurons or nerve fibers below and above the implanted site remained unaffected. It is worth noting that an interface stable for six months in rats may remain functional for years in humans, due to reduced foreign body reactions and impedance values, as reported in the literature.

The patchiness of information related to the interaction of neurons and interfaces has limited the use of intra-neural implants in clinical applications, although they have been used in several research studies on humans. None of the human studies went beyond the limit of four weeks, due to the penetrating nature of these interfaces. They did, however, show interactions with multiple neurons that could be selectively recorded for use in controlling multiple functions of a prosthesis. In one human study, complete termination of the sensory signals was observed after 10 d of implantation due to foreign body reactions [65]. As mentioned in the previous section, these interfaces have been implanted in several studies that succeeded in getting useful motor signals, but the durations of the studies were very limited, from days to a month. This does not provide adequate information related to the stable and long-term use of penetrating-type interfaces. (In a different study, intramuscular and epimysial interfaces were implanted in human subjects and successfully used to provide upper-limb function for over 16 years [112], but these implants were not peripheral nerve interfaces.)

In comparison to the above-mentioned studies, a study was conducted in which extra-neural (spiral cuff) interfaces were implanted in 14 human subjects with spinal cord injuries or upper limb amputation for a period of more than ten years [113]. The key outcomes examined were activation thresholds, muscle recruitment curves, and percent overlap of recruited motor unit populations. Stable thresholds were observed at several interface sites. After six years of implantation, the muscle selectivity of two multi-contact spiral cuffs was still high.

The results of this study and some of the studies discussed in the preceding section [49–54] have shown the potential of extra-neural implants to be used clinically in human peripheral nerves for long periods of time in a stable and selective manner. However, the regular use of extra- or intra-neural implants for prosthetic control has yet to be achieved due to several issues, including the limited rate of information transfer, limited stability of the acquired signals, limited biocompatibility of the interface, inability of the interface to provide sensory feedback, and lack of overall system robustness. Another important issue is that very few research groups have been working on implanted peripheral nerve interfaces and their application in humans. Along with this, the need for permission from health administrative authorities can be a barrier to long-term implantation. Consequently, most of the decoding studies have lasted less than a month, which is sufficient to demonstrate the usability of an interface but not its long-term viability (although this has been demonstrated in animal studies). Moreover, the cooperation of the amputee is also an extremely important factor, because he or she has already experienced a traumatic event.

Many control signals must be recorded, transmitted, and processed in a short time to operate a multifunctional prosthesis. To address this need, several decoding algorithms have been implemented in the past to increase the responsiveness of a prosthesis and enhance its intuitive control. In the next section, we will review peripheral nerve signal decoding processes using the most recently developed algorithms and methods for feature extraction and classification.

6. Peripheral nerve signal decoding processes

Two types of signals can be attained from peripheral nerves, population activity, and spike activity. As explained in the signal acquisition section, population activity signals can be recorded using extra-neural interfaces such as a cuff or FINE, which are placed around a nerve. In these cases, the recorded signals carry information about overall nerve activity rather than neuron-specific information. Spike activity signals, on the other hand, can be recorded using intra-neural interfaces such as LIFE or TIME and their variants, as well as MEAs. These interfaces are placed inside the nerve, either laterally or transversely. Hence, the recorded signals are action potentials (spikes) carrying the electrical information passing through individual nerve fibers (axons). The raw ENG signals have low amplitude and relatively high noise levels, and generally need to be denoised prior to further processing [114].

6.1. Preprocessing

6.1.1. Sources of noise. Common sources of noise in ENG signals include EMG, transient artifacts, oscillatory or time-varying noise, motor nerve signals in transected axons, and

other distortions [14]. These sources of noise are inherent; this fact necessitates the application of filters to raw signals before further processing.

6.1.2. Filters. Many different methods have been used to filter raw ENG signals. Some of the most popular are common average reference [115] for removal of EMG artifacts, thresholding for removal of transient low-amplification noise, band-pass filters for oscillatory noise, adaptive filters for time-varying noise due to the inherent nature of nerve signals, and de-trending of signals for removal of baseline voltage shifts [116]. Deeper processing makes use of Bayesian spatial filters for source signal extraction algorithm [9] and a hybrid extension of this approach [117] that simultaneously maximizes the SNR of the source signal and minimizes cross-talk [118]. These methods can precisely separate peripheral neural signals, potentially providing the voluntary, nearly natural, robust command signals needed for advanced prosthetic limbs.

Wavelet denoising is a technique used in signal processing for simultaneously manipulating both the time and frequency components of a signal. It is used to remove noise as well as to detect features, for enhanced classification performance. The signal is first transformed into an orthogonal time-frequency representation. Thresholding is applied to the transformed coefficients, and the signal is then converted back into the original domain, thereby yielding denoised data. For signals comprising spikes, modified wavelet-denoising [119] and classification [120] algorithms have been used for accurate detection of action potentials from a nerve. Another study [114] used finite impulse response (FIR) bandpass filters to extract the required frequency band and to effectively remove all noise outside of it. A method based on the stationary wavelet transform for denoising spike signals and improving action potential detection has also been developed [121]. For each potential mother wavelet, the researchers thresholded the amplitude of the output signal to detect action potentials. Spikes were detected based on a threshold value obtained after inverse transformation. Finally, the wavelet corresponding to the highest root mean square of the average was selected as the optimal mother wavelet. Using a wavelet filter (wavelet multi-level decomposition and reconstruction) before detecting spikes improved the SNR, preserved the shape of the waveform, and increased cluster discrimination [122].

For population activity signals, optimal filters (Wiener, Matched, and band pass filters) have been designed that improved the SNR by 137% for the Wiener, 211% for the Matched, and 203% for the band pass filter [123]. Assuming the noise to be Gaussian and the signal to be non-Gaussian, the researchers were able to extract, as action-potential peaks, signal amplitudes exceeding the value of the estimated noise amplitude. These analyses made it clear that the modality selectivity of ENG recordings can be increased using optimal filtering. These results can help in understanding how neural activity can be used as a control signal in neural prosthetic devices.

6.2. Channel selection and reduction

Continuous multi-dimensional electrophysiological signals are of high density, and therefore computationally expensive. Processing them requires substantial computing power and fast algorithms, making systems costly and difficult to implement. Moreover, these signals sometimes have linear dependencies, which can reduce their classification performance. Dimensionality reduction algorithms such as mutual information-based or correlation-based channel selection, principal components analysis, or independent component analysis can be helpful in tackling this type of problem.

6.2.1. Principal component analysis (PCA). PCA is a statistical technique that uses variance to convert overlapping data into non-overlapping data via orthogonal transformation. This technique, which is very popular in neural-signal analysis, has been reported extensively in the literature [35, 85, 124–129]. PCA can transform a set of data with correlated values to a set of values that are linearly uncorrelated, called principal components. The highest-order principle components have the largest levels of variability; each subsequent principal component has lower variability. The PCA algorithm uses eigenvalue techniques for correlation calculation. For highly correlated data, the eigenvalues of the correlation matrix show a large disparity, implying a small number of meaningful principal components (transformed signals). In such a case, the rest of the components can be ignored. After transformation, the resulting data set has lower dimensionality, which means reduced complexity and easier classifiability.

If Σ is the covariance matrix of the entire set of neural data x, with eigenvector matrix α and eigenvectors α_k corresponding to eigenvalues λ_k, the equation

$$\max\left(\text{var}\left[\alpha^T x\right]\right) = \alpha_1^T \sum \alpha_1 = \lambda_1, \tag{1}$$

can be used to find the largest eigenvalue λ_1, which gives the first principle component. This process can be continued in a similar manner to find the subsequent principal components. Generally, the first four or five principal components are used in neural data analysis.

6.3. Source extraction

Neural data obtained from population activity recordings may contain signals from both motor and sensory sources. To utilize the acquired signal effectively in a neural-signal-controlled system, it is useful to determine its source. A beamforming algorithm has been developed that uses prior knowledge of the cuff interface geometry for source separation [130]. The advantage of this algorithm is that it does not assume signal independence, nor does it require an extensive knowledge of the nerve geometry. This algorithm requires two training stages. Afterwards, a realistic finite element model is used for validation of the resulting algorithm, based on a more realistic model of the nerve. For recordings from the human
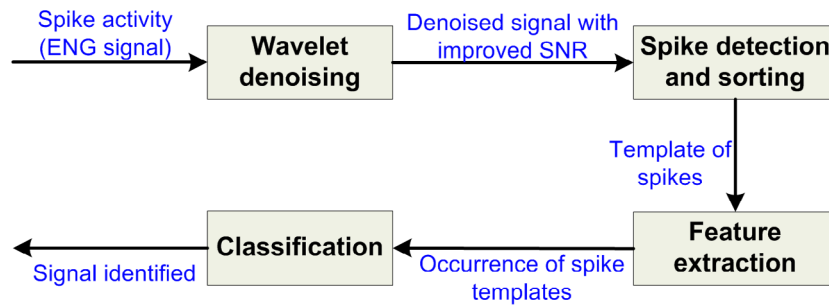
Figure 3. Flowchart of a general spike sorting algorithm.

femoral nerve, the algorithm was able to separate signals from sources as close together as 1.5 mm and with cross-correlation coefficients $R > 0.9$.

Another source extraction algorithm has been developed and tested using cuff interface signals, called blind source separation [131]. This was used in recovering independent source signals from recordings (using FINE) of mixed signals. The recorded mixed signal is decomposed in the form

$$x(t) = As(t) + g(t), \qquad (2)$$

where A is the mixing matrix, $s(t)$ is the original source signal, and $g(t)$ is the recorded noise. The estimated source signal $c(t)$ is given by the equation

$$c(t) = Wx(t), \qquad (3)$$

where W is an estimated demixing matrix obtained by optimizing an objective function which implicitly measures the degree of mutual independence in the estimated source signals.

Using fast-independent component analysis, an objective function was developed as

$$J(x) \approx k_1(\varepsilon\{G_1(x)\})^2 + k_2(\varepsilon\{G_2(x)\} - \varepsilon\{G_2(v)\})^2, \qquad (4)$$

where $G_1(x) = (1/a_1)\log\cosh(a_1 x)$, $G_2(x) = -e^{-x^2/2}$, v is a Gaussian random variable, and $1 \leqslant a_1 \leqslant 2$.

Correlation coefficients were calculated by quantifying the similarities between original fascicular sources and the estimated sources. The researchers were able to recover four independent fascicular sources from six simulated channel recordings with correlation coefficients $R > 0.95$.

6.4. Feature extraction

Raw action potential signals from the PNS are rarely used directly for decoding of movement intentions. Intra-neural interfaces record spikes that can be processed using spike sorting algorithms, but for population activity recorded using extra-neural interfaces, different types of features need to be extracted. Both scenarios are discussed in the following sections.

6.4.1. Spike detection and sorting.

A typical active motor neuron generates 40–200 action potentials per second. Spikes are normally detected in recorded data using some form of thresholding, and may be further sorted based on the spike waveform. Because different types of axons can yield different spike shapes, the shape of a spike can be helpful in determining which type of motor activity is associated with the recorded signal. For this purpose, spike-sorting algorithms are used. This is a very popular to decoding neural data from the PNS [10, 82, 85, 132–136]. The spike-sorted data can be used to decode neural information as well as to determine the onset of activity in a nerve unit.

The spike sorting process consists of two phases. First, the recorded spikes are grouped into clusters based on the similarity of their shapes. Before the second step, noise removal is useful—a popular technique for noise removal in spike sorting algorithms is wavelet denoising (WD) [119–122, 137], though the Butterworth band pass filter can also be used. After denoising, the spikes are aligned, typically with respect to the amplitude peaks. In the second step, templates for different spike shapes are generated, either directly or in the form of features, and then spikes with similar features are grouped into clusters that hopefully correspond to different neurons. The flow diagram for a typical spike sorting algorithm is shown in figure 3.

PCA and wavelet transforms are commonly used for dimensionality reduction in spike sorting. PCA yields an efficient coding of spikes, as only the first two to three principal components usually need to be retained (for mathematical details on PCA, see section 6.2.1). However, it may require offline training along with high computational cost and hardware resources, with no guarantee of optimal separation of clusters. The wavelet transform (WT) is a multi-resolution algorithm that provides good time resolution at high frequencies and good frequency resolution at low frequencies. However, the convolution of the wavelet function with the original signal requires multiple multiplications and additions per spike, resulting in a high computational cost.

Spike detection is done by comparing the denoised signal to a detection threshold and extracting a time window around each peak that rises above the threshold. In one study [114], the detection threshold was chosen to be three times the standard deviation of the samples in each window. However, this method is sensitive to non-Gaussian noise. Another study [120] has proposed a more robust threshold selection process based on the nonlinear energy operator (NEO):

$$\eta\{\hat{x}[k]\} = \hat{x}^2[k] - \hat{x}[k+1] \cdot \hat{x}[k-1]. \qquad (5)$$

The threshold is chosen as a scaled version (scaled by an empirically chosen variable C) of the mean value of NEO.

$$\text{Thr} = C \frac{1}{N} \sum_{k=1}^{N} \eta \{\hat{x}[k]\}. \tag{6}$$

After extraction, the spikes are sorted and labeled according to their shape and size.

A spike sorting algorithm based on PCA and subtractive clustering has been developed [138]. Spike templates (i.e. waveforms) were created according to the clustering results for recordings from a microelectrode array. A template-matching procedure was used in which the minimum residual variance was computed by comparing each spike event with time-shifted versions of each template. If the residual variance passed a Chi-squared test, the spike was labeled as matching the best-fitting template. The formula used was

$$\frac{(W-1)\,v^2}{\sigma^2} \sim \chi^2\,(W-1), \tag{7}$$

where W is the length of the waveform sample, v is the variance of the residue (the difference between the spike waveform and the time-shifted template), and σ is the variance of the non-spiking period. This method was able to reduce the problem of overfitting as well as decreasing the computational cost.

Another algorithm, convolutive independent component analysis, was developed for unsupervised spike sorting from recordings made with high density microelectrodes. Bayesian model estimation was utilized by this method to assess the spatiotemporal structure of the data and avoid overfitting. Reduced spike overlaps were achieved along with increased SNR. A continuous-wavelet-transform-based spike-detection algorithm was developed that used the correlation between wavelet coefficients at different sampling scales to create a robust spike detector [139]. Another similar algorithm was proposed and tested for spike sorting and detection on data recorded from *in vitro* 2D neural networks. This method was based on wavelet packet decomposition [140].

Feature extraction is often carried out on recordings to improve classification. Some of the most commonly used features in spike sorting are as follows: PCA coefficients, wavelet transform (localizes distinctive spike features, with superparamagnetic clustering) [141], first and second derivative extrema and geometric features [82], spike rates of each waveform [114], spike height and width or peak-to-peak amplitude [142], kurtosis [143], correlation coefficients, mean squared difference values, power or energy of a spike [64], repolarization slope [144], and geometric shape of the spike waveform [145].

6.4.2. Feature extraction for population-activity signal. Characteristic features can also be generated for population activity signals, to increase the classifiability of the data as well as reduce dimensionality, thus making data analysis less computationally expensive. A common type of feature used in decoding behavior from population signals is the power in discrete frequency bands. Several types of features can be extracted from an ENG signal, including time-based [41] and phase-based features [146]. During feature extraction, to enhance the information in the ENG signal, the time-series is divided

into optimal length samples referred to as the running observation window (ROW). The features are extracted within this window, thereby preserving the temporal characteristics of the data. To avoid mishandling data at the boundaries, the windows are overlapped by a certain percentage. The size of the ROWs and percentage of overlap play an important role in determining classification performance and are generally dependent on the paradigm and the features being extracted. In experiments using an extra-neural interface placed around the sciatic nerve of anesthetized rats, different ROWs were tested, ranging from 25 to 300 ms, with overlap ranging from 25% to 75%. Various features were tested, including mean absolute values, variance unbiased estimator, wavelength [97], wavelet denoising, energy band on discrete Fourier transform, autoregression coefficients [147], Cepstral coefficients [148], and autocorrelation-based features [149]. Mathematical descriptions of some features used extensively in the literature are shown in table 1.

6.5. Classification technique

Classification techniques are used to categorize the nerve signals generated by a prosthesis user. These categorized signals are then translated into control commands for application interface purposes. Both the sorted spikes and population-activity features are passed to classification algorithms for determination of user intent. A wide variety of algorithms have been tested for ENG and EMG signals, including support vector machines (SVM) [41, 63, 64], artificial neural networks [65], Kalman filters [89], genetic algorithms [150], and Bayesian methods. Clustering is also a very popular machine learning method used for neural signals; various methods including K-means, fuzzy-C means, and density-based clustering [82] have been applied. Some of the classification techniques used in the past are discussed below.

6.5.1. Support vector machines. SVM is a very popular pattern recognition technique for biomedical signals and has been used in several studies [8, 114]. This technique can settle on a global minimum error after training. In addition, it is repeatable and fast, thus popular for use in on-chip systems. It is a supervised binary classifier [151] that determines the 'maximum margin hyperplane', a hyperplane that gives the maximum class separation. The algorithm does this by mapping the input data into a feature space that can be divided using linear or non-linear decision boundaries, depending on its kernel functions (Gaussian or radial basis functions) [24]. For a multi-class problem, the data are subdivided into multiple two-class problems and a one-against-one approach is used [152]. For an n-class classification problem, $n(n-1)/2$ machines can be trained. The open source library LIBSVM [153] is extensively used for applications of SVM.

6.5.2. Kalman filter-based decoding. Neural signals obtained from a population of neurons such as those acquired by epi-neural interfaces or MEAs contain information that can be used to generate movement estimates. These estimates can vary continuously over a range of possible movements, such as arm or hand movements, including grip patterns [84].

Table 1. Overview of features extracted from literature on peripheral nerve signals.

Feature	Description	Definition
Mean absolute value [41]	Measures mean absolute value of a signal in fixed sized windows	$\bar{X} = \frac{1}{N} \sum_{k=1}^{N} |x_k|$
Variance [41]	Determines the (squared) deviation of the data from the mean value	$\sigma^2 = \frac{1}{N} \sum_{k=1}^{N} (x_k - \mu)^2$
Willison amplitude (WAMP) [97]	Counts number of times the signal crosses a set threshold value	$\text{WAMP} = \sum_{k=1}^{N} f\left(|x_k - x_{k+1}|\right)$
Autoregressive features [41]	Accounts for the stochastic nature of nerve signals	$x_i = \sum_{k=1}^{N} a_k x_{i-k}$
Extrema sampling of discrete derivatives [10]	Calculate the slope of data points and extract the min and max values	$DD_t(i) = x(i) - x(i-t)$
Haar based wavelet transform [141]	Time-frequency representation of the signal	$W_{\psi} X(a,b) = \langle x(t) | \psi_{a,b}(t) \rangle$ $\psi_{a,b}(t) = |a|^{-\frac{1}{2}} \psi\left(\frac{t-b}{a}\right)$
Geometric features [127]	Calculates the positive and negative signal energy	$E_s = \int_{-\infty}^{\infty} s^2(t) \mathrm{d}t$
Wavelet coefficients [127]	Decomposes the signals into mutually orthogonal set of wavelets at different scales given by 'a'	$\frac{1}{\sqrt{|a|}} \int_{-\infty}^{\infty} \psi\left(\frac{u-t}{a}\right) f(u) \, \mathrm{d}(u)$
Repolarization slope (RPS) [144]	Determines the magnitude of the slope of the spike in the region in which it falls most rapidly, called repolarization	$r = \max_n \left\{ \sum_{-\infty}^{\infty} x[n+m] \, p[m] \right\}$
NEO Coefficients [120]	Calculates the energy content of the signal at time n.	$\psi(x[n]) = x^2[n] - x[n-1] \, . \, x[n+1]$

Continuous decoding methods such as Kalman filtering (KF) can be used to decode and reconstruct the intended movement. Hand movement patterns have been decoded using KF [89]. According to the researchers who did this, as a first approximation a linear relationship between hand kinematics and the neural data was assumed in the algorithm.

The linear temporal relation between hand movements x can be given by [14]

$$x_{k+1} = Ax_k + w_k, \tag{8}$$

where A is the predictor matrix for the state variable, and w is the prediction error vector. Similarly, the relation between the hand kinematics and the neural signal z can be represented as

$$z_k = Hx_k + q_k, \tag{9}$$

where H is the coefficient matrix and q is the modeling error vector. The vectors w and q are assumed to be Gaussian, with zero mean and orthogonal covariance matrix. The Kalman decoder estimates the movement vector x_k at time t_k, given the observation vector z_k and knowledge of the matrices A and H.

6.5.3. Clustering. Clustering techniques organize unlabeled data into groups to maximize within-class similarities and minimize between-class similarities. An ideal clustering algorithm for online analysis should be automatic, non-parametric and able to classify without *a priori* knowledge.

6.5.3.1. K-means clustering. Spikes are assigned to clusters based on the minimum Euclidean distance between the data points and the centroid of the cluster [140]. The main benefit of this method in spike sorting is that the algorithm is very simple and fast [127].

6.5.3.2. Fuzzy C-means clustering. Spikes are assigned to all clusters according to their degree of membership, depending on the Euclidean distance from the cluster centroid and the degree of fuzziness [154]. In the 'defuzzification' step, a spike is classified according to its maximum membership value.

6.5.3.3. Density-based clustering. In the training phase, a density distribution is calculated from the feature space. Each detected spike results in an increase in the density of its corresponding and surrounding feature cells. After computing the density distribution of the training spikes, labels are given to the cells according to a local density maximum. Finally, the entire density map is separated in an unsupervised way into several clusters corresponding to the local density peaks.

6.5.3.4. Bayesian clustering. In Bayesian clustering, each cluster is modeled with a multivariate Gaussian centered on the cluster. Classification is performed by calculating the probability p of a data point belonging to a cluster:

$$p(c_k|x, \theta_{1:k}) = \frac{p(x|c_k, \theta_k) \, p(c_k)}{\sum_k p(x|c_k, \theta_k) \, p(c_k)}, \tag{10}$$

where $\theta_{1:k} = \{\mu_1, \ \Sigma_1, ..., \ \mu_k, \ \Sigma_k\}$, μ_k is the mean, Σ_k is the covariance matrix for class c_k, and $p(c_k)$ corresponds to the relative firing frequencies.

6.5.3.5. O-sort clustering. O-sort clustering [126] is an online, automatic, and unsupervised algorithm. It starts by assigning the first data point to a cluster of its own. After that, the distance between the next data point and each cluster centroid is computed. A threshold value called the merging threshold is set based on the standard deviation. If the smallest distance is less than the merging threshold, the data point is assigned to the nearest cluster; otherwise it is used to start a new cluster. The mean of the updated clusters is recalculated at every step, and the process is repeated as many times as required. This

algorithm is adaptive, hence non-stationarity of data in time can cause movement of the clusters and changes in the number of clusters. A weakness of this method is that it may split clusters into spurious subclusters, leading to a reduction in clustering performance.

7. Performance evaluation and validation

The feasibility and effectiveness of the chosen features and classification algorithm can be determined by setting up performance evaluation criteria, such as the percentage of correct classifications. This helps in quantifying the success of the developed system. The performance evaluation criterion used in one study for the classification accuracy of spike sorting techniques was [10]:

$$\text{Classification accuracy} = \frac{\text{True postive}}{\text{Total number of detected spikes}} \times 100\%. \tag{11}$$

Another study calculated a confusion matrix to identify subsets of classes for checking misclassification in the system they developed [114]. The overall percentage of correct classifications (PC) was calculated as the ratio of the number of trials whose stimulus type was correctly identified to the total number of trails classified. A validation scheme was also set up in that study to ensure that test and training data remain free of bias.

In another evaluation scheme, the results of spike sorting are assessed based on *a priori* knowledge of the input [124]. Two measures were used; (i) the ratio of the number of clusters output by the spike sorting procedure to the actual number of clusters, (ii) the number of false positive and false negative spikes for each cluster versus the number of spikes that should have been assigned to each cluster. The general cluster percentage error was defined as

$$\text{Cluster error}(n_e) = \frac{F_n(n_e) + F_p(n_e)}{\sum_{n_e=1}^{e} S(n_e) + S_{\text{NOISE}}} \times 100\%, \tag{12}$$

where n_e is a member of a set of expected clusters ($n_e = 1,\ldots,e$), $F_n(n_e)$ and $F_p(n_e)$ are the numbers of false negative and false positive spikes respectively, $S(n_e)$ is the number of spikes truly belonging to each cluster, and S_{NOISE} is the expected number of overlapping spikes.

In another study [82], the rate of classification accuracy was defined as the ratio of the number of correctly classified spikes to the total number of input spikes. Cluster validity (CV), the ratio of between-cluster to within-cluster distance, was used as an index of performance, along with intra-cluster variance (ICV), to determine the probability of misclassification in each cluster. The formulas used were

$$\text{CV} = \frac{\min\limits_{i=1..K, j=1..K} \|CC_i - CC_j\|^2}{\sum_{i=1}^{K} \sum_{A \in N_i} \frac{\|A - CC_i\|^2}{N}}, \tag{13}$$

where CC_i and CC_j are the centers of clusters *i and j* respectively, N is the total number of spikes, K is the number of neurons simulated in the recording, and A is the feature vector; and

$$\text{ICV}_i = \frac{1}{N_i} \sum_{j=1}^{N_i} \|v_j - \mu_i\|^2, \tag{14}$$

where v_j is the *j*th spike in the *i*th cluster, μ_i is its mean template and N_i is the number of spikes in cluster *i*.

8. Online systems for decoding of peripheral nerve signals

The most obvious application of a nerve-controlled interface system is prosthetic devices used as replacements for an upper limb. The system would translate nerve signals into useful motor commands for driving the prostheses. For optimal naturalness and practicality, the developed system must be online, real-time, and autonomous [126, 155]. This requires that the algorithms developed are computationally inexpensive, robust, and suitable for hardware implementation. Correspondingly, the hardware should be compact and power-efficient. To enable naturalistic prosthetic control, data must be continuously streamed from the implanted device in real time and with minimal latency. One method of doing this is to apply feature extraction to limit the amount of data that needs to be transmitted [156]. For example, from the detected neuronal spikes, only the active portion of data may be transmitted, which may lead to an order of magnitude reduction of the required (useful) data rate. Another simple, power-efficient method for reducing the data rate while preserving spike timing information has also been used [157]: spike detection was performed by detecting threshold crossings with a comparator and a user-programmable threshold voltage, and the comparators were reset roughly once per millisecond, which provides sufficient temporal resolution and results in a total data rate of $100 \, \text{kb} \, \text{s}^{-1}$ for all channels. To solving the problem of circuit wiring, the electronic module was surface-mounted directly onto the electrode's flat substrate [158].

8.1. Amplification

Development of a low-noise, low-power amplifier is important for hardware realization. It must be capable of amplifying neural signals in the range of 500–5000 Hz while rejecting large direct current (DC) offsets generated at the intersection of tissue with the implanted interface. An 8 μW fully integrated CMOS biological amplifier was developed for this purpose [159]. Using this system, the researchers were able to achieve an ultralow-frequency response while completely rejecting large DC offsets. A programmable amplification component was added to exploit the full dynamic range of the device in an *in vivo* experiment using an intra-neural interface [160]. Recently, a compact, low powered, current mode neural spike detector was developed for neural recording applications based on an approximation of the non-linear energy operator [161].

8.2. Algorithm optimization for hardware implementation

For implementation of neural decoding algorithms in embedded systems for online applications, the algorithms must be optimized for real-time operation and low power consumption. For example, Zamani and Demosthenous [10] developed a simplified model of the discrete wavelet transform in which they computed discrete derivatives by calculating the slope at each sample point over a number of different time scales. O-sort clustering was employed, as it provides real-time mapping of spikes to single-neuron activity and was able to reduce the data rate to about 0.2% of the original data rate, thus reducing computational complexity. In fact, a very low data rate is especially advantageous in a high-channel-count-recording micro-system [162].

Wavelet denoising and spike detection, as well as a classification algorithm, were optimized in a study of real-time decoding of neural signals [120]. The neuro-prosthetic application in that study was developed on a DSP platform. The researchers used a binary trigger to label the data during training, along with a use of soft-margin version of SVM for easier optimization, thereby reducing the computational cost.

9. Discussion and future work

Neuroprosthetics holds great promise for restoration of function and sensation to people who have lost limbs. Improvements in robustness, longevity, and effectiveness will lead to the development of more intuitive and natural devices capable of meeting the day-to-day requirements of people with amputations. Although upper-limb prosthetic technology has existed for several decades, it is only recently, with advancements in microelectronics and other technological and scientific developments, that it has become possible to realize true neuro-prostheses. With the development of diverse types of interfaces, researchers now have a variety of ways of acquiring peripheral nerve signals, which can be adapted to individual patient requirements. However, there are several points of concern that have yet to be addressed, including the need for an implanted interface for recording and stimulation to have the following properties: (i) biocompatibility or bio-integrability; (ii) long-term stability, selectivity and reliability of the interface and the signals it produces; (iii) ability to communicate bidirectionally; (iv) manageable cost and complexity; (v) sense of embodiment for the user; (vi) ability to provide near-natural feelings, phantom pain relief, and improved psychological well-being for an amputee. Providing sensory feedback using peripheral nerve stimulation is a critical requirement of prosthesis users. The practical complications and shortcomings of interfaces are both biological and biophysical. These challenges include: nerve injury during interface implantation; stability issues in the interface over time due to inflammation; reliability of the interface in terms of functional resolution; relatively weak, noisy electrical signals causing incorrect interpretation of neural signals; implantation-associated injury to nerve axons; and long-term biocompatibility of interfaces.

Although many useful results have been obtained (as explained especially in section 5), challenges still lie ahead. First, several sensory information (tactile feedback) should be used for better control of prostheses. This feedback can be generated using sophisticated stimulation methods that are able to fully exploit the potential of neural interfaces. For example, Tyler and colleagues [53] have shown that several sensations can be evoked using patterned complex electrical stimulations that activate afferent neurons in a more natural way than simple electrical impulses. Micera and colleagues [163] also have demonstrated the ability of subjects to discriminate sophisticated textural features using intra-neural stimulation. Despite these advances, over the next few years the main challenge will be to achieve long-term stable implants for large-scale clinical applications. Several approaches have long been studied, based on which the primary goal is to fabricate an interface that is stable and biocompatible and that can selectively record signals from the peripheral nerve to drive a prosthesis. To achieve this, it will be essential to develop new implant materials that provide more intimate and more natural interfaces with the peripheral nervous system, and to perform long-term tests of their biocompatibility and stability.

For the current state of the art in neural interfaces, it is difficult to judge longevity, because most of the clinical trials have lasted less than a month, due largely to constraints imposed by regulatory authorities. In addition, it can be difficult to convince an amputee who has already experienced a traumatic event to undergo surgery and a long period of interface implantation. Moreover, breakage of the interface within or outside of the nerve is also one of the problems that need to be solved for long-term implants. A recent study by Wurth and colleagues [111] demonstrated the selectivity, stability, longevity, and biocompatibility of intra-neural type interfaces on animals. Stable detection of movement intent was also demonstrated in another study on animals by Durand and colleagues [151] using an extra-neural (FINE) interface. It will be interesting to see the results of implantation of these interfaces in humans for longer periods. However, evidence has been published for long-term stability of peripheral nerve stimulation for sensory feedback using extra-neural interfaces [53, 113]. To be considered a successful long-term interface, a control system must satisfy the following conditions: (i) simultaneous proportional control of multiple prosthesis functions with intuitive generation of near-natural movements; (ii) robust enough to handle signal deviations with continuous usage and variations in limb position; (iii) can be executed with lowest number of interfaces; (iv) supports a feedback mechanism other than vision; (v) perceived by amputees as part of their body; (vi) able to avoid incorrect classification and undesirable movements; and (vii) the most important, real-time function. With the rapid pace of advances in machine learning and the steadily increasing computational power of embedded systems, processing physiological signals in real time is much more feasible than it was in the past. However, achieving directly nerve-controlled interfaces still requires significant additional research and trials before marketable systems can be designed and built [17].

10. Conclusions

Peripheral nerves provide access to highly processed and seg-regated neural command signals from the brain for the control of skeletal muscles, but the relevant interface technologies are still rather primitive. These primitive interfaces have already been fruitfully used to record motor commands and evoke informative sensations. More sophisticated interfaces could in principle provide lifelike, intuitive control of prosthetic limbs with multiple degrees of freedom. Existing interfaces can be improved by making them more biocompatible and more compliant, thus less damaging to the axons, fascicles, and other parts of a nerve. This paper provides a detailed analysis of the existing interface technologies, the state of the art in decoding, their limitations, and the methods that have been developed and applied by researchers to neuroprosthet-ics, from acquisition of the signal to control of the prosthesis. Depending on the type and site of amputation, researchers can choose the most suitable interface for acquisition of either spike signals or population activity signals. Such signals require machine-learning techniques for decoding, including feature extraction in running time windows and classification to determine appropriate motor commands. This paper addi-tionally discussed the various on-chip deployments of decod-ing schemes that have been used, including their development and the optimization of algorithms that can make them com-putationally efficient for use in real-time systems.

Acknowledgment

ORCID iDs

Keum-Shik Hong ⬤ https://orcid.org/0000-0002-8528-4457

References

[1] ElKoura G and Singh K 2003 Handrix: animating the human hand *Symp. on Computer Animation (San Diego, CA, 26–27 July 2003)* (Switzerland: Eurographics Association) pp 110–9

[2] Vallbo A B and Johansson R S 1984 Properties of cutaneous mechanoreceptors in the human hand related to touch sensation *Hum. Neurobiol.* **3** 3–14

[3] Ciancio A L *et al* 2016 Control of prosthetic hands via the peripheral nervous system *Front. Neurosci.* **10** 116

[4] Vidal G V, Rynes M L, Kelliher Z and Goodwin S J 2016 Review of brain-machine interfaces used in neural prosthetics with new perspective on somatosensory feedback through method of signal breakdown *Scietifica* **2016** 8956432

[5] del Valle J and Navarro X 2013 Interfaces with the peripheral nerve for the control of neuroprostheses *Int. Rev. Neurobiol.* **109** 63–83

[6] Navarro X, Krueger T, Lago N, Micera S, Stieglitz T and Dario P 2005 A critical review of interfaces with the peripheral nervous system for the control of neuroprostheses and hybrid bionic systems *J. Peripher. Nerv. Syst.* **10** 229–58

[7] Ohnishi K, Weir R F and Kuiken T A 2007 Neural machine interfaces for controlling multifunctional powered upper-limb prostheses *Expert Rev. Med. Devices* **4** 43–53

[8] Micera S *et al* 2010 Decoding information from neural signals recorded using intraneural electrodes: toward the development of a neurocontrolled hand prosthesis *Proc. IEEE* **98** 407–17

[9] Tang Y, Wodlinger B and Durand D M 2014 Bayesian spatial filters for source signal extraction: a study in the peripheral nerve *IEEE Trans. Neural Syst. Rehabil. Eng.* **22** 302–11

[10] Zamani M and Demosthenous A 2014 Feature extraction using extrema sampling of discrete derivatives for spike sorting in implantable upper-limb neural prostheses *IEEE Trans. Neural Syst. Rehabil. Eng.* **22** 716–26

[11] Badia J, Pascual-Font A, Vivó M, Udina E and Navarro X 2010 Topographical distribution of motor fascicles in the sciatic-tibial nerve of the rat *Muscle Nerve* **42** 192–201

[12] Micera S, Carpaneto J and Raspopovic S 2010 Control of hand prostheses using peripheral information *IEEE Rev. Biomed. Eng.* **3** 48–68

[13] Micera S and Navarro X 2009 Bidirectional interfaces with the peripheral nervous system *Int. Rev. Neurobiol.* **86** 23–38

[14] Warren D J, Kellis S, Nieveen J G, Wendelken S M, Dantas H, Davis T S, Hutchinson D T, Normann R A, Clark G A and Mathews V J 2016 Recording and decoding for neural prosthesis *Proc. IEEE* **104** 374–91

[15] Farina D and Aszmann O 2014 Bionic limbs: clinical reality and academic promises *Sci. Transl. Med.* **6** 257

[16] Di Pino G *et al* 2014 Invasive neural interfaces: the perspective of the surgeon *J. Surg. Res.* **188** 77–87

[17] Schultz A E and Kuiken T A 2011 Neural interfaces for control of upper limb prostheses: the state of the art and future possibilities *Arch. Phys. Med. Rehabil.* **3** 55–67

[18] Wolpaw J R, Birbaumer N, McFarland D J, Pfurtscheller G and Vaughan T M 2002 Brain-computer interfaces for communication and control *Clin. Neurophysiol.* **113** 767–91

[19] Machado S *et al* 2010 EEG-based brain-computer interfaces: an overview of basic concepts and clinical applications in neurorehabilitation *Rev. Neurosci.* **21** 451–68

[20] Khan M J and Hong K-S 2017 Hybrid EEG-fNIRS-based eight-command decoding for BCI: application to quadcopter control *Front. Neurorobot.* **11** 1–13

[21] Khan M J, Hong M J and Hong K-S 2014 Decoding of four movement directions using hybrid NIRS-EEG brain-computer interface *Front. Hum. Neurosci.* **8** 1–10

[22] Turnip A and Hong K-S 2012 Classifying mental activities from EEG-P300 signals using adaptive neural networks *Int. J. Innov. Comput.* I **8** 6429–43

[23] Pfurtscheller G and Lopes da Silva F H 1999 Event-related EEG/MEG synchronization and desynchronization: basic principles *Clin. Neurophysiol.* **110** 1842–57

[24] Naseer N and Hong K-S 2015 fNIRS-based brain-computer interfaces: a review *Front. Hum. Neurosci.* **9** 172

[25] Bhutta M R, Hong M J, Kim Y-H and Hong K-S 2015 Single-trial lie detection using a combined fNIRS-polygraph system *Front. Psychol.* **6** 709

[26] Khan M J and Hong K-S 2015 Passive BCI based on drowsiness detection: an fNIRS study *Biomed. Opt. Express* **6** 4063–78

[27] Nguyen H-D and Hong K-S 2016 Bundled-optode implementation for 3D imaging in functional near-infrared spectroscopy *Biomed. Opt. Express* **7** 3491–507

[28] Hong K-S and Khan M J 2017 Hybrid brain-computer interface techniques for improved classification accuracy and increased number of commands: a review *Front. Neurorobot.* **11** 35

[29] Hong K-S, Bhutta M R, Liu X and Shin Y I 2017 Classification of somatosensory cortex activities using fNIRS. *Behav. Brain Res.* **333** 225–34

[30] Naseer N and Hong K-S 2016 Reduction of delay in detecting initial dips from functional near-infrared spectroscopy signals using vector-based phase analysis *Int. J. Neural Syst.* **26** 1650012

[31] Zafar A and Hong K-S 2017 Detection and classification of three-class initial dips from prefrontal cortex *Biomed. Opt. Express* **8** 367–83

[32] Hu X-S, Hong K-S and Ge S S, Jeong M-Y 2010 Kalman estimator- and general linear model-based on-line brain activation mapping by near-infrared spectroscopy *Biomed. Eng. Online* **9** 82

[33] Kamran M A and Hong K-S 2014 Reduction of physiological effects in fNIRS waveforms for efficient brain-state decoding *Neurosci. Lett.* **580** 130–6

[34] Kamran M A and Hong K-S 2013 Linear parameter-varying model and adaptive filtering technique for detecting neuronal activities: An fNIRS study *J. Neural. Eng.* **10** 056002

[35] Santosa H, Hong M J, Kim S-P and Hong K-S 2013 Noise reduction in functional near-infrared spectroscopy signals by independent component analysis *Rev. Sci. Instrum.* **84** 073106

[36] Wodlinger B, Downey J E, Tyler-Kabara E C, Schwartz A B, Boninger M L and Collinger J L 2015 Ten-dimensional anthropomorphic arm control in a human brain–machine interface: difficulties, solutions, and limitations *J. Neural Eng.* **12** 016011

[37] Biddiss E, Beaton D and Chau T 2007 Consumer design priorities for upper limb prosthetics *Disabil. Rehabil. Assist. Technol.* **2** 346–57

[38] Agnew W F, McCreery D B, Yuen T G and Bullara L A 1989 Histologic and physiologic evaluation of electrically stimulated peripheral nerve: considerations for the selection of parameters *Ann. Biomed. Eng.* **17** 39–60

[39] Naples G G, Mortimer J T, Scheiner A and Sweeney J D 1988 A spiral nerve cuff electrode for peripheral nerve stimulation *IEEE Trans. Biomed. Eng.* **35** 1140–1

[40] Tyler D J and Durand D M 2002 Functionally selective peripheral nerve stimulation with a flat interface nerve electrode *IEEE Trans. Neural Syst. Rehabil. Eng.* **10** 294–303

[41] Raspopovic S, Carpaneto J, Udina E, Navarro X and Micera S 2010 On the identification of sensory information from mixed nerves using single-channel cuff electrodes *J. Neuroeng. Rehabil.* **7** 17

[42] Boger A, Bhadra N and Gustafson K J 2013 Different clinical electrodes achieve similar electrical nerve conduction block *J. Neural Eng.* **10** 056016

[43] Riso R R, Mosallaie F K, Jensen W and Sinkjaer T 2000 Nerve cuff recordings of muscle afferent activity from tibial and peroneal nerves in rabbit during passive ankle motion *IEEE Trans. Rehabil. Eng.* **8** 244–58

[44] Park H J and Durand D M 2015 Motion control of the rabbit ankle joint with a flat interface nerve electrode *Muscle nerve* **52** 1088–95

[45] Dweiri Y M, Eggers T, McCallum G and Durand D M 2015 Ultra-low noise miniaturized neural amplifier with hardware averaging *J. Neural Eng.* **12** 046024

[46] Yoo P B and Durand D M 2005 Selective recording of the canine hypoglossal nerve using a multicontact flat interface nerve electrode *IEEE Trans. Biomed. Eng.* **52** 1461–9

[47] Badia J, Boretius T, Andreu D, Azevedo-Coste C, Stieglitz T and Navarro X 2011 Comparative analysis of transverse intrafascicular multichannel, longitudinal intrafascicular and multipolar cuff electrodes for the selective stimulation of nerve fascicles *J. Neural Eng.* **8** 036023

[48] Kent A R and Grill W M 2013 Model-based analysis and design of nerve cuff electrodes for restoring bladder function by selective stimulation of the pudendal nerve *J. Neural Eng.* **10** 036010

[49] Polasek K H, Hoyen H A, Keith M W, Kirsch R F and Tyler D J 2009 Stimulation stability and selectivity of chronically implanted multicontact nerve cuff electrodes in the human upper extremity *IEEE Trans. Neural Syst. Rehabil. Eng.* **17** 428–37

[50] Schiefer M A, Polasek K H, Triolo R J, Pinault G C and Tyler D J 2010 Selective stimulation of the human femoral nerve with a flat interface nerve electrode. *J. Neural Eng.* **7** 026006

[51] Schiefer M A, Freeberg M, Pinault G J, Anderson J, Hoyen H, Tyler D J and Triolo R J 2013 Selective activation of the human tibial and common peroneal nerves with a flat interface nerve electrode *J. Neural Eng.* **10** 056006

[52] Tan D W, Schiefer M A, Keith M W, Anderson J R, Tyler J and Tyler D J 2014 A neural interface provides long-term stable natural touch perception *Sci. Trans. Med.* **6** 257ra138

[53] Tan D W, Schiefer M A, Keith M W, Anderson J R and Tyler D J 2015 Stability and selectivity of a chronic, multi-contact cuff electrode for sensory stimulation in human amputees *J. Neural Eng.* **12** 026002

[54] Ortiz-Catalan M, Hakansson B and Branemark R 2014 An osseointegrated human-machine gateway for long-term sensory feedback and motor control of artificial limbs *Sci. Transl. Med.* **6** 257re6

[55] Durand D M 2007 Neural engineering-a new discipline for analyzing and interacting with the nervous system *Methods Inf. Med.* **46** 142–6

[56] Ortiz-Catalan M, Brånemark R, Hakansson B and Delbeke J 2012 On the viability of implantable electrodes for the natural control of artificial limbs: review and discussion *Biomed. Eng. Online* **11** 33

[57] Malagodi M S, Horch K W and Schoenberg A A 1989 An intrafascicular electrode for recording of action potentials in peripheral nerves *Ann. Biomed. Eng.* **17** 397–410

[58] Yoshida K and Horch K 1993 Selective stimulation of peripheral nerve fibers using dual intrafascicular electrodes *IEEE Trans. Biomed. Eng.* **40** 492–4

[59] Dhillon G S, Lawrence S M, Hutchinson D T and Horch K W 2004 Residual function in peripheral nerve stumps of amputees: implications for neural control of artificial limbs *J. Hand Surg. Am.* **29** 605–15

[60] Dhillon G S and Horch K W 2005 Direct neural sensory feedback and control of a prosthetic arm *IEEE Trans. Neural Syst. Rehabil. Eng.* **13** 468–72

[61] Horch K, Meek S, Taylor T G and Hutchinson D T 2011 Object discrimination with an artificial hand using electrical stimulation of peripheral tactile and proprioceptive pathways with intrafascicular electrodes *IEEE Trans. Neural Syst. Rehabil. Eng.* **19** 483–9

[62] Lago N, Yoshida K, Koch K P and Navarro X 2007 Assessment of biocompatibility of chronically implanted polyimide and platinum intrafascicular electrodes *IEEE Trans. Biomed. Eng.* **54** 281–90

[63] Micera S *et al* 2008 On the use of longitudinal intrafascicular peripheral interfaces for the control of cybernetic hand prostheses in amputees *IEEE Trans. Neural Syst. Rehabil. Eng.* **16** 453–72

[64] Micera S, Rossini P M, Rigosa J, Citi L, Carpaneto J, Raspopovic S, Tombini M, Cipriani C, Assenza G and Carrozza M 2011 Decoding of grasping information from

neural signals recorded using peripheral intrafascicular interfaces *J. Neuroeng. Rehabil.* **8** 53

[65] Rossini P M, Micera S, Benvenuto A, Carpaneto J, Cavallo G, Citi L, Cipriani C, Denaro L, Denaro V and Di Pino G 2010 Double nerve intraneural interface implant on a human amputee for robotic hand control *Clin. Neurophysiol.* **121** 777–83

[66] Boretius T, Badia J, Pascual-Font A, Schuettler M, Navarro X, Yoshida K and Stieglitz T 2010 A transverse intrafascicular multichannel electrode (TIME) to interface with the peripheral nerve *Biosens. Bioelectron.* **26** 62–9

[67] Badia J, Raspopovic S, Carpaneto J, Micera S and Navarro X 2016 Spatial and functional selectivity of peripheral nerve signal recording with the transversal intrafascicular multichannel electrode(TIME) *IEEE Trans. Neural Syst. Rehabil. Eng.* **24** 20–7

[68] Badia J, Boretius T, Pascual-Font A, Udina E, Stieglitz T and Navarro X 2011 Biocompatibility of chronically implanted transverse intrafascicular multichannel electrode (TIME) in the rat sciatic nerve *IEEE Trans. Biomed. Eng.* **58** 8

[69] Kundu A, Wirenfeldt M, Harreby K R and Jensen W 2014 Biosafety assessment of an intra-neural electrode (TIME) following sub-chronic implantation in the median nerve of Göttingen minipigs *Int. J. Artif. Organs* **37** 466–76

[70] Kundu A, Harreby K R, Yoshida K, Boretius T, Stieglitz T and Jensen W 2014 Stimulation selectivity of the 'thin-film longitudinal intrafascicular electrode' (tfLIFE) and the 'transverse intrafascicular multi-channel electrode' (TIME) in the large nerve animal model *IEEE Trans. Neural Syst. Rehabil. Eng.* **22** 400–10

[71] Lefurge T, Goodall E, Horch K, Stensaas L and Schoenberg A 1991 Chronically implanted intrafascicular recording electrodes *Ann. Biomed. Eng.* **19** 197–207

[72] Yoshida K, Jovanović K and Stein R B 2000 Intrafascicular electrodes for stimulation and recording from mudpuppy spinal roots *J. Neurosci. Methods* **96** 47–55

[73] Lawrence S M, Dhillon G S, Jensen W, Yoshida K and Horch K W 2004 Acute peripheral nerve recording characteristics of polymer-based longitudinal intrafascicular electrodes *IEEE Trans. Neural Syst. Rehabil. Eng.* **12** 345–8

[74] Li L-J, Zhang J, Zhang F, Lineaweaver W C, Chen T-Y and Chen Z-W 2005 Longitudinal intrafascicular electrodes in collection and analysis of sensory signals of the peripheral nerve in a feline model *Microsurgery* **25** 561–5

[75] Yoshida K, Farina D, Akay M and Jensen W 2010 Multichannel intraneural and intramuscular techniques for multiunit recording and use in active prostheses *Proc. IEEE* **98** 432–49

[76] Rossini P M, Rigosa J, Micera S, Assenza G, Rossini L and Ferreri F 2011 Stump nerve signals during transcranial magnetic motor cortex stimulation recorded in an amputee via longitudinal intrafascicular electrodes *Exp. Brain Res.* **210** 1–11

[77] Zheng X, Zhang J, Chen T and Chen Z 2003 Longitudinally implanted intrafascicular electrodes for stimulating and recording fascicular physioelectrical signals in the sciatic nerve of rabbits *Microsurgery* **23** 268–73

[78] Zheng X, Zhang J, Chen T and Chen Z 2008 Recording and stimulating properties of chronically implanted longitudinal intrafascicular electrodes in peripheral fascicles in an animal model *Microsurgery* **28** 203–9

[79] Raspopovic S, Capogrosso M, Petrini F M, Bonizzato M, Rigosa J, Di Pino G, Carpaneto J, Controzzi M, Boretius T and Fernandez E 2014 Restoring natural sensory feedback in real-time bidirectional hand prostheses *Sci. Trans. Med.* **6** 222ra19

[80] Aoyagi Y, Stein R B, Branner A, Pearson K G and Normann R A 2003 Capabilities of a penetrating microelectrode array for recording single units in dorsal root ganglia of the cat *J. Neurosci. Methods* **128** 9–20

[81] McDonnall D, Clark G A and Normann R A 2004 Selective motor unit recruitment via intrafascicular multielectrode stimulation *Can. J. Physiol. Pharmacol.* **82** 599–609

[82] Regalia G, Coelli S, Biffi E, Ferrigno G and Pedrocchi A 2016 A framework for the comparative assessment of neuronal spike sorting algorithms towards more accurate off-line and on-line microelectrode arrays data analysis *Comput. Intell. Neurosci.* 8416237

[83] Mirfakhraei K and Horch K 1997 Recognition of temporally changing action potentials in multiunit neural recordings *IEEE Trans. Biomed. Eng.* **44** 123–31

[84] Stark E and Abeles M 2007 Predicting movement from multiunit activity *J. Neurosci.* **27** 8387–94

[85] Leibig C, Wachtler T and Zeck G 2016 Unsupervised neural spike sorting for high-density microelectrode arrays with convolutive independent component analysis *J. Neurosci. Methods* **271** 1–13

[86] Ledbetter N M, Ethier C, Oby E R, Hiatt S D, Wilder A M, Ko J H, Agnew S, Miller L and Clark G 2013 Intrafascicular stimulation of monkey arm nerves evokes coordinated grasp and sensory responses *J. Neurophysiol.* **109** 580–90

[87] Branner A, Stein R B and Normann R A 2001 Selective stimulation of cat sciatic nerve using an array of varying-length microeletrodes *J. Neurophysiol.* **85** 1585–94

[88] Christensen M B, Pearce S M, Ledbetter N M, Warren D J, Clark G A and Tresco P A 2014 The foreign body response to the utah slant electrode array in the cat sciatic nerve *Acta Biomater.* **10** 4650–60

[89] Davis T S, Wark H A C, Hutchinson D T, Warren D J, O'Neill K, Scheinblum T, Clark G, Normann R and Greger B 2016 Restoring motor control and sensory feedback in people with upper extremity amputations using arrays of 96 microelectrodes implanted in the median and ulnar nerves *J. Neural Eng.* **13** 036001

[90] Byun D, Cho S J, Lee B H, Min J, Lee J H and Kim S 2017 Recording nerve signals in canine sciatic nerves with a flexible penetrating microelectrode array *J. Neural Eng.* **14** 046023

[91] Akin T, Najafi K, Smoke R H and Bradley R M 1994 A micromachined silicon sieve electrode for nerve regeneration applications *IEEE Trans. Biomed. Eng.* **41** 305–13

[92] Wallman L, Zhang Y, Laurell T and Danielsen N 2001 The geometric design of micromachined silicon sieve electrodes influences functional nerve regeneration *Biomaterials* **22** 1187–93

[93] Lacour S P, Fitzgerald J J, Lago N, Tarte E, McMahon S and Fawcett J 2009 Long micro-channel electrode arrays: a novel type of regenerative peripheral nerve interface *IEEE Trans. Neural Syst. Rehabil. Eng.* **17** 454–60

[94] Fitzgerald J J, Lago N, Benmerah S, Serra J, Watling C P, Cameron R E, Tarte E, Lacour S, McMahon S and Fawcett J 2012 A regenerative microchannel neural interface for recording from and stimulating peripheral axons *in vivo J. Neural Eng.* **9** 016010

[95] Navarro X, Calvet S, Rodriguez C, Stieglitz T, Blau C, Buti M, Valderrama E and Meyer J U 1998 Stimulation and recording from regenerated peripheral nerves through polyimide sieve electrodes *J. Periph. Nerv. Syst.* **3** 91–101

[96] Hargrove L J, Englehart K and Hudgins B 2007 A comparison of surface and intramuscular myoelectric signal classification *IEEE Trans. Biomed. Eng.* **54** 847–53

[97] Zecca M, Micera S, Carrozza M C and Dario P 2002 Control of multifunctional prosthetic hands by processing the electromyographic signal *Crit. Rev. Biomed. Eng.* **30** 459–85

[98] Scott R N and Parker P A 1988 Myoelectric prostheses:state of the art *J. Med. Eng. Technol.* **12** 143–51

[99] Merletti R, Holobar A and Farina D 2008 Analysis of motor units with high-density surface electromyography *J. Electromyogr. Kinesiol.* **18** 879–90

[100] Marateb H R, Farahi M, Rojas M, Maanas M A and Farina D 2016 Detection of multiple innervation zones from multi-channel surface EMG recordings with low signal-to-noise ratio using graph-cut segmentation *PLoS One* **11** e0167954

[101] Negro F, Muceli S, Castronovo A M, Holobar A and Farina D 2016 Multi-channel intramuscular and surface EMG decomposition by convolutive blind source separation *J. Neural Eng.* **13** 026027

[102] Pasquina P F *et al* 2015 First-in-man demonstration of a fully implanted myoelectric sensors system to control an advanced electromechanical prosthetic hand *J. Neurosci. Methods* **244** 85–93

[103] Karimimehr S, Marateb H R, Muceli S, Mansourian M, Mananas M A and Farina D 2017 A real-time method for decoding the neural drive to muscles using single-channel intra-muscular EMG recordings *Int. J. Neural syst.* **27** 1750025

[104] Muceli S, Poppendieck W, Negro F, Yoshida K, Hoffman K P, Butler J E, Gandevia S C and Farina D 2015 Accurate and representative decoding of the neural drive to muscles in humans with multi-channel intramuscular thin-film electrodes *J. Physiol.* **593** 3789–804

[105] Ghafoor U, Kim S and Hong K-S 2017 Selectivity and longevity of peripheral nerve and machine interface: a review *Front. Neurorobot.* **10** 59

[106] Reilly K T, Mercier C, Schieber M H and Sirigu A 2006 Persistent hand motor commands in the amputees' brain *Brain* **129** 2211–23

[107] Dhillon G S, Kruger T B, Sandhu J S and Horch K W 2005 Effects of short term training on sensory and motor function in severed nerves of long-term human amputees *J. Neurophysiol.* **93** 2625–33

[108] Gasson M, Hutt B, Goodhew I, Kyberd P and Warwick K 2005 Invasive neural prosthesis for neural signal detection and nerve stimulation *Int. J. Adapt. Control Signal Process.* **19** 365–75

[109] Jia X, Koenig M A, Zhang X, Zhang J, Chen T and Chen Z 2007 Residual motor signal in long-term human severed peripheral nerves and feasibility of neural signal-controlled artificial limb *J. Hand Surg. Am.* **32** 657–66

[110] Grill W M, Norman S E and Bellamkonda R V 2009 Implanted neural interfaces: biochallenges and engineered solutions. *Ann. Rev. Biomed. Eng.* **11** 1–24

[111] Wurth S *et al* 2017 Long-term usability and bio-integration of polyimide based intra-neural stimulating electrodes *Biomaterials* **122** 114–29

[112] Kilgore K L, Peckham P H, Keith M W, Montague F W, Hart R L, Gazdik M M, Bryden A M, Snyder S A and Stage T G 2003 Durability of implanted electrodes and leads in an upper-limb neuroprosthesis *J. Rehabil. Res. Dev.* **40** 457–68

[113] Christie B P, Freeberg M, Memberg W D, Pinault G J C, Hoyen H A, Tyler D J and Triolo R J 2017 Long-term stability of stimulating spiral nerve cuff electrodes on human peripheral nerves *J. Neuroeng. Rehabil.* **14** 70

[114] Citi L, Carpaneto J, Yoshida K, Hoffman K P, Koch K P, Dario P and Micera S 2008 On the use of wavelet denoising and spike sorting techniques to process electroneurographic signals recorded using intraneural electrodes *J. Neurosci. Methods* **172** 294–302

[115] Kelly J W, Siewiorek D P, Smailagic A and Wang W 2013 Automated filtering of common-mode artifacts in multichannel physiological recordings *IEEE Trans. Biomed. Eng.* **60** 2760–70

[116] Bokil H, Andrews P, Kulkarni J E, Mehta S and Mitra P P 2010 Chronux: a platform for analyzing neural signals *J. Neurosci. Meth.* **192** 146–51

[117] Eggers T E, Dweiri Y M, McCallum G A and Durand D M 2017 Model-based Bayesian signal extraction algorithm for peripheral nerves *J. Neural Eng.* **14** 056009

[118] Wodlinger B and Durand D M 2011 Selective recovery of fascicular peripheral nerves *J. Neural Eng.* **8** 056005

[119] Diedrich A, Charoensuk W, Brychta R J, Ertl A C and Shiavi R 2003 Analysis of raw microneurographic recordings based on wavelet de-noising technique and classification algorithm: wavelet analysis in microneurography *IEEE Trans. Biomed. Eng.* **50** 41–50

[120] Pani D, Barabino G, Citi L, Meloni P, Raspopovic S, Micera S and Raffo L 2016 Real-Time Neural Signals decoding onto off-the-shelf DSP processors for neuroprosthetic applications *IEEE Trans. Neural Syst. Rehabil. Eng.* **24** 993–1002

[121] Kamavuako E N, Jensen W, Yoshida K, Kurstjens M and Farina D 2010 A criterion for signal-based selection of wavelets for denoising intrafascicular nerve recordings *J. Neurosci. Methods* **186** 274–80

[122] Wiltschko A B, Gage G J and Berke J D 2008 Wavelet filtering before spike detection preserves waveform shape and enhances single-unit discrimination *J. Neurosci. Methods* **173** 34–40

[123] Jezernik S and Grill W M 2001 Optimal filtering of whole nerve signals *J. Neurosci. Methods* **106** 101–10

[124] Adamos D A, Kosmidis E K and Theophilidis G 2008 Performance evaluation of PCA-based spike sorting algorithms *Comput. Methods Prog. Biomed.* **91** 232–44

[125] Jolliffe I T 2002 *Principal Component Analysis* (New York: Springer)

[126] Rutishauser U, Schuman E M and Mamelak A N 2006 Online detection and sorting of extracellularly recorded action potentials in human medial temporal lobe recordings *in vivo J. Neurosci. Methods* **154** 204–24

[127] Bestel R, Daus A W and Thielemann C 2012 A novel automated spike sorting algorithm with adaptable feature extraction *J. Neurosci. Methods* **211** 168–78

[128] Dowden B R, Frankel M A, Normann R A and Clark G A 2012 Non-invasive method for selection of electrodes and stimulus parameters for FES applications with intrafascicular arrays *J. Neural Eng.* **9** 016006

[129] Aghagolzadeh M and Oweiss K 2009 Compressed and distributed sensing of neuronal activity for real time spike train decoding *IEEE Trans. Neural Syst. Rehabil. Eng.* **17** 116–27

[130] Wodlinger B and Durand D M 2009 Localization and recovery of peripheral neural sources with beamforming algorithms *IEEE Trans. Neural Syst. Rehabil. Eng.* **17** 461–8

[131] Tesfayesus W and Durand D M 2007 Blind source separation of peripheral nerve recordings *J. Neural Eng.* **4** 157–67

[132] Barnett A H, Magland J F and Greengard L F 2016 Validation of neural spike sorting algorithms without ground-truth information *J. Neurosci. Methods* **264** 65–77

[133] Lewicki M S 1998 A review of methods for spike sorting: the detection and classification of neural action potentials *Netw. Comput. Neural Syst.* **9** R53–78

[134] Kim K H and Kim S J 2000 Neural spike sorting under nearly 0 db signal-to-noise ratio using nonlinear energy operator and artificial neural-network classifier *IEEE Trans. Biomed. Eng.* **47** 1406–11

[135] Oweiss K G and Anderson D J 2002 Spike sorting: a novel shift and amplitude invariant technique *Neurocomputing* **44** 1133–9

[136] Shoham S, Fellows M R and Normann R A 2003 Robust, automatic spike sorting using mixtures of multivariate *t*-distributions *J. Neurosci. Methods* **127** 111–22

[137] Stark H-G 2005 *Wavelets and Signal Processing: an Application-based Introduction* (Berlin: Springer)

[138] Zhang P M, Wu J Y, Zhou Y, Liang P J and Yuan J Q 2004 Spike sorting based on automatic template reconstruction with a partial solution to the overlapping problem *J. Neurosci. Methods* **135** 55–65

[139] Yang C, Olson B and Si J 2011 A multiscale correlation of wavelet coefficients approach to spike detection *Neural Comput.* **23** 215–50

[140] Hulata E, Segev R and Ben-Jacob E 2002 A method for spike sorting and detection based on wavelet packets and Shannon's mutual information *J. Neurosci. Methods* **117** 1–12

[141] Quiroga R Q, Nadasdy Z and Ben-Shaul Y 2004 Unsupervised spike detection and sorting with wavelets and superparamagnetic clustering *Neural Comput.* **16** 1661–87

[142] Takahashi S, Anzai Y and Sakurai Y 2003 A new approach to spike sorting for multi-neuronal activities recorded with a tetrode—how ICA can be practical *Neurosci. Res.* **46** 265–72

[143] Brychta R J, Shiavi R, Robertson D and Diedrich A 2007 Spike detection in human muscle sympathetic nerve activity using the kurtosis of stationary wavelet transform coefficients *J. Neurosci. Methods* **160** 359–67

[144] Schwarz D M, Zilany M, Skevington M, Huang N, Flynn B and Carney L H 2012 Semi-supervised spike sorting using pattern matching and a scaled Mahalanobis distance metric *J. Neurosci. Methods* **206** 120–31

[145] Horton P M, Nicol A U, Kendrick K M and Feng J F 2007 Spike sorting based upon machine learning algorithms (SOMA) *J. Neurosci. Methods* **160** 52–68

[146] Canolty R T and Knight R T 2010 The functional role of cross-frequency coupling *Trends Cogn. Sci.* **14** 506–15

[147] Graupe D 1989 EMG pattern analysis for patient-responsive control of FES in paraplegics for walker-supported walking *IEEE Trans. Biomed. Eng.* **6** 711–9

[148] Kang W J, Cheng C K, Lai J S, Shiu J R and Kuo T S 1996 A comparative analysis of various EMG pattern recognition methods *Med. Eng. Phys.* **18** 390–5

[149] Jezernik S, Grill W M and Sinkjaer T 2001 Neural network classification of nerve activity recorded in a mixed nerve *Neurol Res.* **23** 429–34

[150] Cavallaro E, Micera S, Dario P, Jensen W and Sinkjaer T 2003 On the intersubject generalization ability in extracting kinematic information from afferent nervous signals *IEEE Trans. Biomed. Eng.* **50** 1063–73

[151] Dweiri Y M, Eggers T E, Gonzalez-Reyes L E, Drain J, McCallum G A and Durand D M 2017 Stable detection of movement intent from peripheral nerves: chronic study in dogs *Proc. IEEE* **105** 50–65

[152] Huang T K, Weng R C and Lin C J 2006 Generalized Bradley–Terry models and multi-class probability estimates *J. Mach. Learn. Res.* **7** 85–115

[153] Chang C C and Lin C J 2001 *LIBSVM: a Library for Support Vector Machines Software* (https://www.csie.ntu.edu.tw/~cjlin/libsvm/)

[154] Cannon R L, Dave J V and Bezdek J C 1986 Efficient implementation of the fuzzy c-means clustering algorithms *IEEE Trans. Pattern Anal. Mach. Intell.* **8** 248–55

[155] Warwick K, Gasson M, Hutt B, Goodhew I, Kyberd P, Andrews B, Teddy P and Shad A 2003 The application of implant technology for cybernetic systems *Arch. Neurol.* **60** 1369–73

[156] Perelman Y and Ginosar R 2007 An integrated system for multichannel neuronal recording with spike/LFP separation, integrated *A/D* conversion and threshold detection *IEEE Trans. Biomed. Eng.* **54** 130–7

[157] Harrison R R, Watkins P T, Kier R J, Lovejoy R O, Black D J, Greger B and Solzbacher F 2007 A low-power integrated circuit for a wireless 100 electrode neural recording system *IEEE J. Solid-State Circuits* **42** 123–33

[158] Lertmanorat Z, Montague F W and Durand D M 2009 A flat interface nerve electrode with integrated multiplexer *IEEE Trans. Neural Syst. Rehabil. Eng.* **17** 176–82

[159] Harrison R R and Charles C 2003 A low-power low-noise CMOS amplifier for neural recording applications *IEEE J. Solid-State Circuits* **38** 958–65

[160] Loi D, Carboni C, Angius G, Angotzi G N, Barbaro M, Raffo L, Raspopovic S and Navarro X 2011 Peripheral neural activity recording and stimulation system *IEEE Trans. Biomed. Circuits Syst.* **5** 368–79

[161] Yao E, Chen Y and Basu A 2016 A 0.7V, 40 nW compact, current-mode neural spike detector in 65 nm CMOS *IEEE Trans. Biomed. Circuits Syst.* **10** 309–18

[162] Chew D J *et al* 2013 A microchannel neuroprosthesis for bladder control after spinal cord injury in rat *Sci. Transl. Med.* **5** 210ra155

[163] Oddo C M *et al* 2016 Intraneural stimulation elicits discrimination of textural features by artificial fingertip in intact and amputee humans *eLife* **5** e09148